



## Research Article

# Egg-shell Treated Oil Palm Fronds (EG-OPF) as Low-Cost Adsorbent for Methylene Blue Removal

Rosalyya Hasan<sup>1</sup>, Nur Aida Farihin Ahliyasah<sup>1</sup>, Chi Cheng Chong<sup>1</sup>, Rohayu Jusoh<sup>1</sup>,  
Herma Dina Setiabudi<sup>1,2,\*</sup>

<sup>1</sup> Faculty of Chemical and Natural Resources Engineering, Universiti Malaysia Pahang, 26300  
Gambang, Kuantan, Pahang, Malaysia

<sup>2</sup> Centre of Excellence for Advanced Research in Fluid Flow, Universiti Malaysia Pahang, 26300  
Gambang, Kuantan, Pahang, Malaysia

Received: 1<sup>st</sup> October 2018; Revised: 28<sup>th</sup> October 2018; Accepted: 14<sup>th</sup> November 2018;  
Available online: 25<sup>th</sup> January 2019; Published regularly: April 2019

## Abstract

A new adsorbent (egg-shell treated oil palm fronds (EG-OPF)) prepared from wastes was evaluated for methylene blue (MB) removal. Optimization among three significant variables (initial concentration ( $X_1$ ), initial pH ( $X_2$ ), and adsorbent dosage ( $X_3$ )) were executed using response surface methodology (RSM). The most excellent performance was marked at  $X_1 = 291.7$  mg/L,  $X_2 = \text{pH } 5$ , and  $X_3 = 1.82$  g/L, with MB removal of 80.26 %. The kinetic study was fitted perfectly with the pseudo-second-order model ( $R^2 > 0.990$ ), indicating the chemisorption process. The isotherm study was found to follow the Langmuir isotherm model ( $R^2 = 0.999$ ), with maximal adsorption magnitude of 714.3 mg/g, implying the monolayer adsorption on a homogenous adsorbent surface. The reusability study affirmed the feasibility of EG-OPF in MB removal, credited to its excellent performance during reusability studies. The present study successfully discovered a new low-cost adsorbent (EG-OPF) for MB removal. Copyright © 2019 BCREC Group. All rights reserved

**Keywords:** Adsorption; Low-Cost Adsorbent; Optimization; Methylene Blue

**How to Cite:** Hasan, R., Ahliyasah, N.A.F., Chong, C.C., Jusoh, R., Setiabudi, H.D. (2019). Egg-shell Treated Oil Palm Fronds (EG-OPF) as Low-Cost Adsorbent for Methylene Blue Removal. *Bulletin of Chemical Reaction Engineering & Catalysis*, 14 (1): 158-164 (doi:10.9767/bcrec.14.1.3322.158-164)

**Permalink/DOI:** <https://doi.org/10.9767/bcrec.14.1.3322.158-164>

## 1. Introduction

Dyes are one of the most important materials in textile, printing, food, rubber, and paper industries to increase the attractiveness of a product. After Perkin discovered the first synthetic dye in 1856, a vast variety of synthetic dyes were developed to meet the high demand in industries [1,2] and there are around 10,000

different commercial dyes existing worldwide. Methylene blue (MB) is a basic dye that broadly adopted in the dyeing process. During the dyeing processes, around 10-15 % of the MB was discharged [3] and appeared as a problematic concern owing to its toxicity [4]. Thus, it is utmost important to eliminate the MB before being discarded to receiving water.

There are various treatment processes to remove MB including membrane filtration [5], electrochemical treatment [6], and adsorption [7]. Among the above mentioned processes, adsorption has attracted considerable attention

\* Corresponding Author.

E-mail: [herma@ump.edu.my](mailto:herma@ump.edu.my) (H.D. Setiabudi)

Telp: +60-9-5492836, Fax: +60-9-5492889

owing to its simplicity and worth for its economic value [8]. The adsorption processes usually involved the use of activated carbon as an adsorbent, however, there are some drawbacks to this material which involved high manufacturing and regeneration cost [9]. For that reason, researchers tended to replace the existing activated carbon by producing effective adsorbent from either agricultural or industrial solid wastes.

As the major industry in Malaysia, palm oil industry generated approximately 30 million tons of fronds, trunks, empty fruit bunches and leaves per year [10]. The abundance of these wastes generated serious environmental pollution due to improper waste management [11]. Thus, it is advantageous to utilize oil palm frond (OPF) as a new adsorbent for MB removal. It has been reported that the efficiency of the low-cost adsorbent can be improved by alkaline treatment due to the improvement in polarity of the surface and the sorption sites' density [12]. However, alkaline treatment is considered to be costly owing to the high price of the chemical. Thus, the utilization of egg-shell (EG) waste which consists of a high composition of CaCO<sub>3</sub> could consider as an alternative material for alkaline treatment owing to its low cost and availability. Moreover, as far as we are concerned, there is no study has been done on OPF treated by EG to perform an economical and practical approach for MB removal. Thus, in this study, egg-shell treated oil palm fronds (EG-OPF) was evaluated for the MB removal and its performance was optimized using response surface methodology (RSM).

## 2. Materials and Method

### 2.1 Preparation and Characterization of Adsorbent

Oil palm frond (OPF) and eggshells (EG) were collected in Pahang, Malaysia. The OPF was cut into small pieces (10-20 mm), soaked in distilled water (12 h), oven-dried (80 °C, 24 h), followed by crushed and sieved (355-500 μm). Subsequently, the EG were washed with distilled water, oven-dried (80 °C, 24 h) and calcined (950 °C, 3 h). The dried eggshells were grounded and sieved into powder with particles size 355-500 μm. XRF analysis confirmed that calcined EG mainly consists of CaO (97.44 %) as shown in Table 1, which decomposed from CaCO<sub>3</sub> via calcination.

For the pre-treatment of OPF with EG, 8.6 g of calcined EG powder was added to 1 L of water, under constant stirring. During this

process, the CaO contained in calcined EG was converted to Ca(OH)<sub>2</sub> upon contact with H<sub>2</sub>O. Then, 10 g OPF was added into the solution, stirred (room temperature, 4 h), filtered, and oven-dried (80 °C, 24 h) to produce EG-OPF. The functional groups of EG-OPF were characterized using Fourier-transform infrared (FTIR) (Nicolet Is5, Thermo Scientific).

### 2.2 Adsorption Experiments

Initially, MB solution was prepared by dissolving the accurate amount of MB (Merck, C.I. 61734) in deionized water and the pH of the solution was adjusted using sodium hydroxide (NaOH, Merck) or hydrochloric acid (HCl, Merck). A specific amount of EG-OPF was added into MB solution (200 mL) under constant stirring (300 rpm, room temperature). The sample was then withdrawn, centrifuged (3800 rpm, 15 min) and analysed using UV/Vis spectrophotometer (LAMBDA 850, Perkin Elmer). The adsorption capacity (mg/g) and percentage removal were calculated using Equations (1) and (2), respectively.

$$q_t = \left( \frac{C_o - C_t}{m} \right) \times V \quad (1)$$

$$\text{Percentage removal}(\%) = \left( \frac{C_o - C_t}{C_o} \right) \times 100 \quad (2)$$

Where, C<sub>o</sub>(mg/L) and C<sub>t</sub> (mg/L) are the MB concentrations at time zero and at time *t*, respectively, *m* (g) is the mass of EG-OPF, and *V* (L) is the volume of MB solution.

### 2.3 Experimental Design and Optimization

The influences of operating conditions on MB removal were optimized using response surface methodology (RSM) coupled with the face-centered central composite design (FCCCD). The RSM was carried out using Sta-

**Table 1.** Chemical composition in calcined EG

Compound	Composition (%)
CaO	97.44
MgO	0.95
P <sub>2</sub> O <sub>5</sub>	0.49
SiO <sub>2</sub>	0.25
Na <sub>2</sub> O	0.21
Al <sub>2</sub> O <sub>3</sub>	0.09
K <sub>2</sub> O	0.09
Fe <sub>2</sub> O <sub>3</sub>	0.04
Others	0.44

tistica (version 10, Statsoft Inc) with independent variables of the initial concentration of MB ( $X_1$ ), initial pH ( $X_2$ ), and adsorbent dosage ( $X_3$ ). The total number of experiments conducted were 16 runs.

### 2.4 Kinetic and Isotherm Studies

The linearized forms of the kinetic models (pseudo-first-order and pseudo-second-order) that used in this study are represented as follows [13,14].

Pseudo-first-order equation:

$$\ln(q_e - q_t) = \ln q_e - k_1 t \quad (3)$$

Pseudo-second-order equation:

$$\frac{t}{q_t} = \frac{1}{k_2 q_e^2} + \frac{1}{q_e} t \quad (4)$$

Where,  $q_e$  (mg/g) is the adsorption capacity at equilibrium,  $q_t$  (mg/g) is the adsorption capacity at time  $t$ ,  $k_1$  (L/min) is the pseudo-first-order constant, while  $k_2$  (L/min) is the pseudo-second-order constant. Meanwhile, the linearized forms of the isotherm models (Freundlich and Langmuir) that used in this study are presented as follows [15,16]:

Freundlich isotherm:

$$\log q_e = \log K_f + \frac{1}{n} \log C_e \quad (5)$$

Langmuir isotherm:

$$\frac{C_e}{q_e} = \frac{1}{q_m K_L} + \frac{C_e}{q_m} \quad (6)$$

Where,  $q_e$  (mg/g) is the adsorption capacity at equilibrium,  $K_f$  ((mg/g).(L/mg)<sup>1/n</sup>) is the Freundlich equilibrium constant,  $n$  is the heterogeneity factor, and  $C_e$  (mg/L) is the MB concentration at equilibrium. Meanwhile,  $K_L$  (L/mg) is the Langmuir constant,  $q_m$  (mg/g) is the maximum adsorption capacity, and  $C_e$  (mg/L) is the MB concentration at equilibrium.

## 3. Result and Discussion

### 3.1 Characteristic of Adsorbent

The functional group present on the surface of OPF, fresh EG-OPF, and spent EG-OPF (MB-EG-OPF) were illustrated in Figure 1. A broad peak was detected around 3320 and 3310 cm<sup>-1</sup> for OPF and EG-OPF, respectively, which ascribed to the O–H stretching mode of hydroxyl groups [17]. The small peaks around 2330 cm<sup>-1</sup> attributed to the C–H stretching

mode of CH<sub>3</sub> and CH<sub>2</sub> groups [18], while a peak detected around 1030 cm<sup>-1</sup> ascribed to the C≡H and C=H. Additionally, a peak detected at 1610 cm<sup>-1</sup> for OPF was ascribed to the C=O stretching mode of carbonyl group [19]. It was observed that the peak at 1610 cm<sup>-1</sup> was shifted to 1420 cm<sup>-1</sup>, indicating the presence of aromatics groups in EG-OPF. The functional groups involved in the MB adsorption was confirmed by the changes in the intensity and wavenumber of several peaks significantly at 3310, 2330, 1420, and 1035 cm<sup>-1</sup>. Thus, it is affirmed that the functional groups of EG-OPF have served to be the active sites for the dye-adsorbent interaction to facilitate the adsorption process.

### 3.2 Statistical Analysis

The experimental design and its results are tabulated in Table 2, while the regression model is given in Equation (7).

$$Y = -75.3453 + 40.9755X_1 + 43.3118X_2 + 0.1079X_3 - 3.1739X_1X_2 - 0.0175X_1X_3 + 0.0255X_2X_3 - 3.0180X_1^2 - 9.5961X_2^2 - 0.0001X_3^2 \quad (7)$$

The ANOVA results, shown in Table 3, confirmed the significance of the model by the greater value of calculated  $F$ -value ( $F_{model} = 17.36$ ) in comparison with the tabulated  $F$ -value ( $F_{0.05} = 1.409$ ).

In addition, a high value of  $R^2$  (0.9630) in parity plot (Figure 2(A)) revealed the good correlation of the model. The Pareto chart shown in Figure 2(B) discovered that the quadratic term of initial pH ( $X_2^2$ ), interaction term of initial pH and adsorbent dosage ( $X_2X_3$ ), interaction term of initial concentration and initial pH ( $X_1X_2$ ), linear term of adsorbent dosage ( $X_3$ ), linear term of initial pH ( $X_2$ ), and quadratic term of adsorbent dosage ( $X_3^2$ ) were statisti-

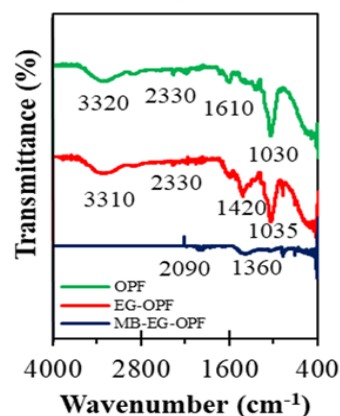


Figure 1. FTIR spectra of OPF, EG-OPF, and MB-EG-OPF

cally significant due to the large  $t$ -value magnitude and small  $p$ -value ( $p < 0.05$ ). The rest of the variables terms were considered less significant, due to a high  $p$ -value ( $p > 0.05$ ). The quadratic term of initial pH ( $X_2^2$ ) was found to be the more prominent variable that highly influenced the MB adsorption onto EG-OPF while the initial concentration ( $X_1$ ) was the least prominent variable.

Figure 3 displays 3D plots for the influences of independent variables on MB removal. As shown in Figure 3(A), an incline in the initial MB concentration and initial pH values simultaneously increased the MB removal until the optimum condition was achieved, and decreased at elevated values. At low initial MB concentration, the quantity of available active sites for adsorption is relatively high, thus increased the MB removal. However, with increasing of MB concentration, the quantity of

available active sites were insufficient to accommodate the superfluous MB ions [4]. For the influence of initial pH, the changes in MB removal associated with the changes in the surface properties and thus influences the ionization and dissociation of the MB molecule [20].

Figure 3(B) revealed that the interaction between initial concentration and adsorbent dosage was less significant in the MB removal onto EG-OPF, in agreement with result observed by Pareto chart (Figure 2(B)). Figure 3(C) displays the influences of initial pH and adsorbent dosage on MB removal. An increase in initial pH and adsorbent dosage significantly increased the MB removal until the optimum condition (pH = 4.9-7 and adsorbent dosage = 1.0-2.0 g/L) was achieved and decreased at higher values. This behavior was related to the basic nature of MB, whereby in acidic con-

**Table 2.** Experimental design of MB removal onto OPF

Run	Manipulated variables						Response
	Initial Concentration, $X_1$ (mg/L)		Initial pH, $X_2$		Adsorbent dosage, $X_3$ (g/L)		MB Removal, $Y$ (%)
	Uncoded	Coded	Uncoded	Coded	Uncoded	Coded	
1	50	-1	2	-1	0.25	-1	10.05
2	400	+1	2	-1	0.25	-1	9.61
3	50	-1	8	+1	2.5	+1	28.15
4	400	+1	8	+1	2.5	+1	69.33
5	50	-1	2	-1	0.25	-1	55.53
6	400	+1	2	-1	0.25	-1	39.83
7	50	-1	8	+1	2.5	+1	52.29
8	400	+1	8	+1	2.5	+1	35.20
9	225	0	5	0	1.375	0	48.68
10	225	0	5	0	1.375	0	57.74
11	225	0	2	-1	0.25	-1	64.95
12	225	0	8	+1	2.5	+1	71.52
13	50	-1	5	0	1.375	0	77.57
14	400	+1	5	0	1.375	0	76.13
15	225	0	5	0	1.375	0	80.27
16	225	0	5	0	1.375	0	80.27

**Table 3.** ANOVA analysis for MB removal onto EG-OPF

Sources	Sum of square (SS)	Degree of freedom (d.f)	Mean Square (MS)	F-Value
Regression (SSR)	7951.08	9	883.45	17.36
Residual	305.38	6	50.90	
Total (SST)	8256.46	15		

dition, the positively charged ions of MB ( $H^+$ ) tend to oppose the cationic EG-OPF adsorption. Meanwhile, in a basic medium, the positively charged ions of MB ( $H^+$ ) tend to interact with the negatively charged adsorbent, resulting in an increase in MB removal [21]. At constant pH, an increase in MB removal with increasing of adsorbent dosage owing to the greater active sites that available for the adsorbent-solute interaction for adsorption.

The process optimization modeling using RSM suggested that the optimal MB removal onto EG-OPF (at 291.71 mg/L MB concentration, pH 5, and 1.82 g/L Eg-OPF) is 81.96 %. To validate the optimization result, an additional experiment was executed and the corresponding result was obtained at 80.26 %.

### 3.3 Kinetic and Isotherm Studies

The kinetic parameters for MB removal onto EG-OPF were listed in Table 4. According to Table 4, the experimental data fitted well with the pseudo-second-order kinetic model ( $R^2 > 0.990$ ), indicating chemisorption process with the rate of reaction was directly proportional to the number of the active sites.

Table 5 shows the isotherm parameters for MB removal onto EG-OPF. According to Table

5, the adsorption of MB onto EG-OPF was found to follow the Langmuir isotherm model ( $R^2 = 0.999$ ), implying the monolayer adsorption on a homogenous adsorbent surface. The obtained  $R_L$  value (0.012) confirmed the favorable MB adsorption [22].

### 3.5 Reusability Study

The reusability study was carried out during five adsorption cycle whereby the spent EG-OPF was filtered and oven-dried (80 °C, 12 h) before being used in the next cycle. As can be observed from Figure 4, EG-OPF shows good performance in MB removal even at the 5<sup>th</sup> cycle of the adsorption process. A slight decrease in adsorption performance during multiple adsorption cycles was related to the existence of MB molecules on the adsorbent surface through chemical bonding after each adsorption process [23].

## 4. Conclusion

EG-OPF was prepared and used as an adsorbent for MB removal. The optimum conditions were achieved at 291.71 mg/L MB concentration, pH 5, and 1.82 g/L EG-OPF. FTIR results confirmed the important role of functional

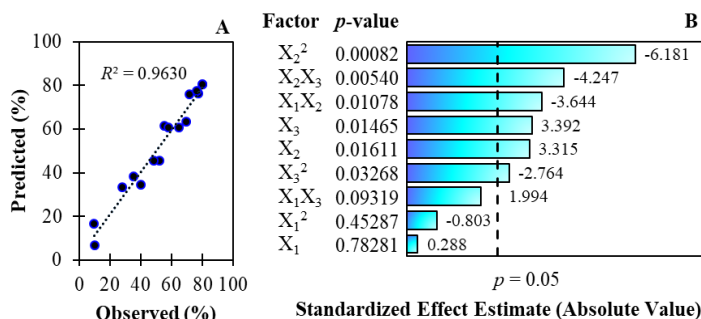


Figure 2. (A) Parity plot and (B) Pareto chart of MB removal onto EG-OPF

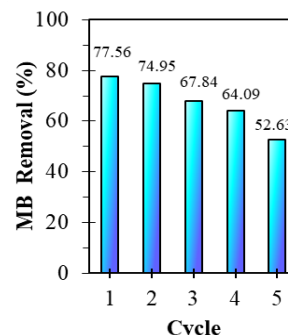


Figure 4. Performance of EG-OPF during five adsorption cycles

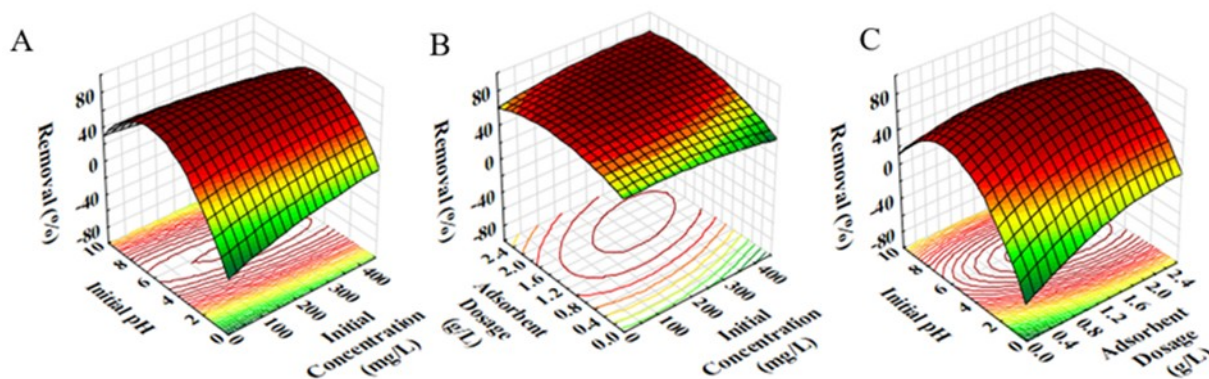


Figure 3. 3D plots of MB removal vs. (A) initial MB concentration and initial pH, (B) initial MB concentration and adsorbent dosage, (C) initial pH and adsorbent dosage

**Table 4.** Kinetic parameters for MB removal onto EG-OPF

Concentration (mg/L)	Experimental	Pseudo-first-order			Pseudo-second-order		
	$q_{m,exp}$ (mg/g)	$q_m$ (mg/g)	$k_1$ (min <sup>-1</sup> )	$R^2$	$q_m$ (mg/g)	$k_2$ (min <sup>-1</sup> )	$R^2$
50	79.26	2.272	0.002	0.401	78.74	0.009	0.999
100	153.6	7.222	0.047	0.990	158.73	0.001	0.998
200	283.3	8.395	0.070	0.980	303.03	0.001	0.990
300	386.8	12.01	0.035	0.940	400.00	0.003	0.991
400	469.0	7.979	0.009	0.423	476.19	0.006	0.995

groups in MB adsorption. Adsorption isotherm study revealed that the MB removal onto EG-OPF fitted well with Langmuir isotherm ( $R^2 = 0.999$ ) with  $q_m = 714.3$  mg/g, indicating the monolayer adsorption on a homogenous adsorbent surface. Adsorption kinetic study discovered that the MB removal onto EG-OPF followed the pseudo-second-order kinetic ( $R^2 > 0.990$ ), indicating the chemisorption process. The feasibility of EG-OPF in MB removal was confirmed by its good activity during five adsorption cycles. This study successfully develops new low-cost adsorbent from waste materials (EG and OPF) for MB removal.

**Acknowledgement**

This project was financially supported by the Universiti Malaysia Pahang (UMP) through Research University Grant (RDU170331).

**References**

[1] Konicki, W., Aleksandrak, M., Moszyński, D., Mijowska, E. (2017). Adsorption of Anionic Azo-Dyes from Aqueous Solutions onto Graphene Oxide: Equilibrium, Kinetic and Thermodynamic Studies. *Journal of Colloid and Interface Science*, 496188-496200.

[2] Tan, K.B., Vakili, M., Horri, B.A., Poh, P.E., Abdullah, A.Z., Salamatinia, B. (2015). Adsorption of Dyes by Nanomaterials: Recent Developments and Adsorption Mechanisms. *Separation and Purification Technology*, 150229-150242.

[3] Sharma, Y.C., Uma. (2010). Optimization of Parameters for Adsorption of Methylene Blue on a Low-Cost Activated Carbon. *Journal of Chemical & Engineering Data*, 55(1): 435-439.

[4] Pathania, D., Sharma, S., Singh, P. (2017). Removal of Methylene Blue by Adsorption onto Activated Carbon Developed from Ficus Carica Bast. *Arabian Journal of Chemistry*, 10S1445-S1451.

**Table 5.** Isotherm parameters for MB removal onto EG-OPF

Isotherm	Parameters	Value
Freundlich	$n$	1.557
	$K_f$ (mg/g)(L/mg) <sup>1/n</sup>	3.601
	$R^2$	0.989
Langmuir	$q_m$ (mg/g)	714.3
	$K_L$ (L/mg)	0.459
	$R^2$	0.999
	$R_L$	0.012

[5] Alventosa-deLara, E., Barredo-Damas, S., Alcaina-Miranda, M.I., Iborra-Clar, M.I. (2012). Ultrafiltration Technology with a Ceramic Membrane for Reactive Dye Removal: Optimization of Membrane Performance. *Journal of Hazardous Materials*, 209: 210492-210500.

[6] Körbahti, B.K., Artut, K., Geçgel, C., Özer, A. (2011). Electrochemical Decolorization of Textile Dyes and Removal of Metal Ions from Textile Dye and Metal Ion Binary Mixtures. *Chemical Engineering Journal*, 173(3): 677-688.

[7] Hassani, A., Alidokht, L., Khataee, A.R., Karaca, S. (2014). Optimization of Comparative Removal of Two Structurally Different Basic Dyes Using Coal as a Low-Cost and Available Adsorbent. *Journal of the Taiwan Institute of Chemical Engineers*, 45(4): 1597-1607.

[8] Tehrani-Bagha, A.R., Nikkar, H., Mahmoodi, N.M., Markazi, M., Menger, F.M. (2011). The Sorption of Cationic Dyes onto Kaolin: Kinetic, Isotherm and Thermodynamic Studies. *Desalination*, 266(1): 274-280.

[9] Setiabudi, H.D., Jusoh, R., Suhaimi, S.F.R.M., Masrur, S.F. (2016). Adsorption of Methylene Blue onto Oil Palm (Elaeis Guineensis) Leaves: Process Optimization, Isotherm, Kinetics and Thermodynamic Studies. *Journal of the Taiwan Institute of Chemical Engineers*, 63363-63370.



- [10] Sumathi, S., Chai, S.P., Mohamed, A.R. (2008). Utilization of Oil Palm as a Source of Renewable Energy in Malaysia. *Renewable and Sustainable Energy Reviews*, 12(9): 2404-2421.
- [11] Saadon, N., Razali, N., Yashim, M.M., Yusof, N.A. (2006). Adsorption of Methylene Blue Using Oil Palm (*Elaeis Guaneensis*) Fronds as Activated Carbon. *ARPN Journal of Engineering and Applied Sciences*, 11(9): 6192-6194.
- [12] Djilali, Y., Elandaloussi, E. H., Aziz, A., Menorval L. C. (2016). Alkaline Treatment of Timber Sawdust: A Straightforward Route toward Effective Low-Cost Adsorbent for the Enhanced Removal of Basic Dyes from Aqueous Solutions. *Journal of Saudi Chemical Society*, 20: S241-S249.
- [13] Lagergren, S. (1898). About the Theory of So-Called Adsorption of Soluble Substances. *Journal of Chemical Engineering*, 24(1): 1-39.
- [14] Ho Y.S., McKay, G. (1999). Pseudo-Second Order Model for Sorption Processes. *Process Biochemistry*, 34(5): 451-465.
- [15] Langmuir, I. (1918). The Adsorption of Gases on Plane Surfaces of Glass, Mica and Platinum, *Journal of the American Chemical Society*, 40: 1361-1403.
- [16] Freundlich, H. (1906). Adsorption in Solution, *The Journal of Physical Chemistry*, 57: 47-385.
- [17] Pradeep Sekhar, C., Kalidhasan, S., Rajesh, V., Rajesh, N. (2009). Bio-Polymer Adsorbent for the Removal of Malachite Green from Aqueous Solution. *Chemosphere*, 77(6): 842-847.
- [18] Teas, C., Kalligeros, S., Zankos, F., Stournas, S., Lois, E., Anastopoulos, G. (2001). Investigation of the Effectiveness of Absorbent Materials in Oil Spills Clean Up. *Desalination*, 140(3): 259-264.
- [19] Marín, A.B.P., Ortuño, J.F., Aguilar, M.I., Meseguer, V.F., Sáez, J., Lloréns, M. (2010). Use of Chemical Modification to Determine the Binding of Cd(II), Zn(II) and Cr(III) Ions by Orange Waste. *Biochemical Engineering Journal*, 53(1): 2-6
- [20] Banerjee, S., Chattopadhyaya, M.C. (2017). Adsorption Characteristics for the Removal of a Toxic Dye, Tartrazine from Aqueous Solutions by a Low Cost Agricultural by-Product. *Arabian Journal of Chemistry*, 10S1629-S1638.
- [21] Pirok, B.W.J., Knip, J., van Bommel, M.R., Schoenmakers, P.J. (2016). Characterization of Synthetic Dyes by Comprehensive Two-Dimensional Liquid Chromatography Combining Ion-Exchange Chromatography and Fast Ion-Pair Reversed-Phase Chromatography. *Journal of Chromatography A*, 1436141-1436146.
- [22] Chatterjee, S., Kumar, A., Basu, S., Dutta, S. (2012). Application of Response Surface Methodology for Methylene Blue Dye Removal from Aqueous Solution Using Low Cost Adsorbent. *Chemical Engineering Journal*, 181: 182289-182299.
- [23] Auta, M., Hameed, B.H. (2014). Chitosan-Clay Composite as Highly Effective and Low-Cost Adsorbent for Batch and Fixed-Bed Adsorption of Methylene Blue. *Chemical Engineering Journal*, 237352-237361.

*Selected and Revised Papers from The 4<sup>th</sup> International Conference of Chemical Engineering & Industrial Biotechnology (ICCEIB 2018) (<http://icceib.ump.edu.my/index.php/en/>) (Universiti Malaysia Pahang, by 1<sup>st</sup>-2<sup>nd</sup> August 2018) after Peer-reviewed by Scientific Committee of ICCEIB 2018 and Peer-Reviewers of Bulletin of Chemical Reaction Engineering & Catalysis*